# Modeling and characterization of InGaAsP selective-area growth with broad bandgap tuning in S- and C-band

Z. Chen, F. Lemaitre, A. Kapoor, P.J. van Veldhoven, Y. Wang, M. Lodde, R. Ma, D.W. Feyisa, K.A. Williams, J.J.G.M. van der Tol and Y. Jiao

Institute for Photonic Integration, Eindhoven University of Technology, PO Box 513, 5600MB, Eindhoven, The Netherlands

*We report a broad bandgap tuning of InGaAsP quantum wells using MOVPE selective-area growth (SAG). A 100 nm photoluminescence wavelength tuning range has been observed. The growth rate enhancement of InGaAsP MQWs have been numerically modelled via the vapor-phase diffusion (VPD) model, and experimentally characterized by surface profiling, revealing good consistency between simulated and experimental results. Beyond 100 nm bandgap wavelengths tunning have been determined via photoluminescence spectroscopy.*

## Introduction

Selective-area growth (SAG) technique is a versatile bandgap engineering approach, which enables multiple wavelengths integration on wafer-scale with only one step of epitaxy. SAG technique has been employed to simplify the monolithic integration of optoelectronic devices with different operation wavelengths on various platforms [1-3].

The bandgap of quantum wells is mainly dependent on the quaternary compound composition, strain and the structure geometry (i.e., the layer thickness). To achieve local bandgap variation, inhomogeneity on the precursor distribution is deliberately introduced to the reaction region by pre-depositing dielectric patterns on the wafer. Since epitaxy can only take place on the crystalline surface and cannot occur on the amorphous dielectric mask surface, a gradient of the precursor concentration is generated near the dielectric mask/semiconductor boundary, and the precursor diffuses from the masked region (dense) to the unmasked region (sparse), causing a concentration increment near the dielectric mask. In metalorganic vapor-phase epitaxy (MOVPE), the growth rate depends linearly on the concentration of the group III precursor in the vapor phase in the immediate vicinity of the surface [4]. Therefore, an enhancement in growth rate and thus an increment in layer thickness at a certain location is achieved. The resulting bandgap energy of the quantum wells (QWs) is thus inversely proportional to the thickness of the QW layer [5]. Besides, the compound composition can also be changed due to the different diffusion lengths of the III group elements.

In this work, we present a beyond 100-nm wavelength engineering in S- and C- band, from 1470 nm to 1575 nm detected by photoluminescence spectroscopy, by applying SAG technique on TU/e's InGaAsP/InP membrane platform [6] for the first time.

## Modeling

In MOVPE process, the diffusion of the vapor phase precursors can be modeled by a Laplace equation with respect to the concentration, i.e., the so-called vapor phase diffusion model (VPD) [7]. The study region that simulates the vapor-phase diffusion in the vicinity of the semiconductor surface, including the boundary conditions, is shown in Fig. 1(a). The study region is 100 μm in height (y-direction) and 1000 μm in length (x-direction). A pair of dielectric stripes (grey) are patterned on the semiconductor surface (blue).

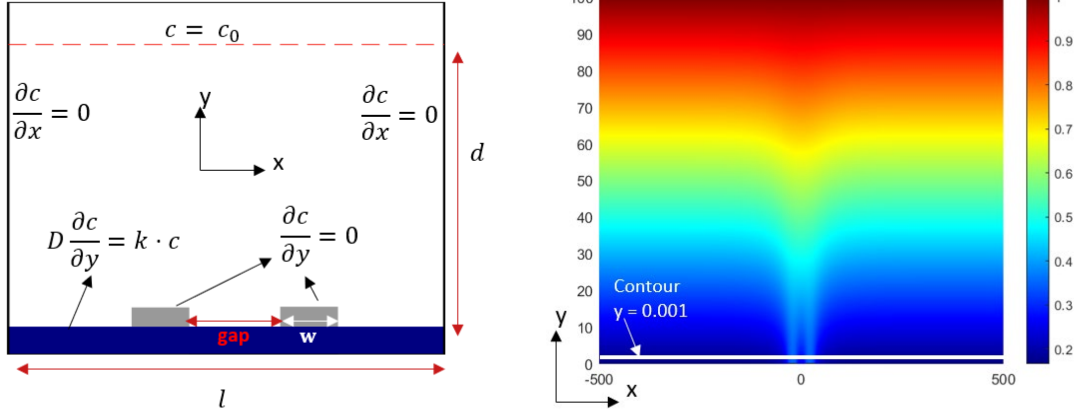


Fig. 1: a.(left) the study region of the VPD model with clarified boundary conditions; b.(right) an illustrative example of the simulated concentration distribution in the study region, with mask width $w = 20$ µm, mask gap $g = 20$ µm and effective diffusion length $D/k = 25$ µm.

The Laplace equation

$$D\left(\frac{\partial^2 c}{\partial x^2} + \frac{\partial^2 c}{\partial y^2}\right) = 0 \quad (1)$$

with boundary conditions

$$c(y = d) = c_0 \quad (2a) \qquad \frac{\partial c}{\partial x}(x = 0; x = l) = 0 \quad (2b)$$

$$D\frac{\partial c}{\partial y} = k \cdot c \text{ , on semicondcutor} \quad (2c) \qquad \frac{\partial c}{\partial y} = 0 \text{ , on mask} \quad (2d)$$

can mathematically describe concentration distribution in the study region. $D$ is the vapor phase diffusion constant, $c$ is the concentration of the III group precursors, $k$ is the (1st order) reaction constant. The concentration at the top edge of the study region is set as constant $c_0$ in Eq. (2a). Eq. (2b) indicates the symmetric and periodic assumption (in x-direction) on the study region. Eq. (2c) describes the diffusion flux balance on the semiconductor surface, while Eq. (2d) reveals the fact that epitaxy cannot happen on amorphous mask surface.

The distribution of the precursor in the study region can be simulated by solving Eq. (1) with boundary conditions (Eq. 2a-2d) with the finite element method (FEM). Simulations show that the concentration distribution is not only influenced by the mask geometry (in this case, the mask width w and the mask gap g) but also related to the surface properties and the growth conditions (temperature, pressure, etc.), which are represented by the effective diffusion length, $D/k$, for simplicity. An illustrative example of the simulation result is plotted in Fig. 1(b), in which the precursor concentration at the top edge ($c_0$) is normalized as 1, each mask stripe is 20 µm wide and the effective diffusion length ($D/k$) is 25 µm. To numerically describe the growth enhancement between the mask stripes caused by SAG in simulation, a dedicated normalized figure of merit, i.e., growth rate enhancement (GRE) is introduced, which is defined as the ratio of the precursor concentration at the center of the mask stripes (where $x = 0$, $y = 0.001$ µm) and the concentration at the uninfluenced region, i.e., the edge of the study region (where $x = \pm 500$ µm, $y = 0.001$ µm), denoted as R,

$$R = \frac{c(x=0, y=0.001)}{c(x=\pm 500, y=0.001)}.$$

In general, larger masks with narrower gap in between bring stronger perturbation to the homogeneity of the precursor distribution, therefore higher growth rate enhancement, since the growth rate is linearly dependent on the precursor concentration in the vapor phase. A quasi-

linear relation between GRE and mask geometry is revealed in Fig. 2. It also illustrates that high diffusion length can degrade the GRE.

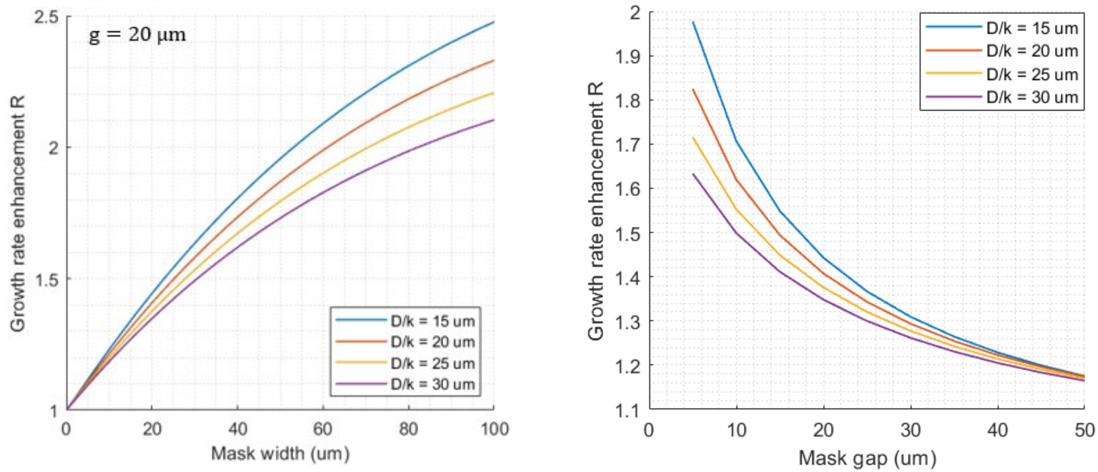


Fig. 2: Simulated GRE as a function of a.(left) mask width and b.(right) mask gap

## Experiment

A standard multiple quantum wells (MQWs) with two separate-confinement heterostructure (SCH) layers is grown on a SiO2-patterned InP wafer under standard growth conditions in an AIXTRON MOVPE reactor. SiO2 is patterned by electron-beam lithography (EBL) using a negative e-beam resist. After development, a two-step etching method (partially RIE dry-etch + partially HF wet-etch) is performed to transfer the pattern from the e-bam resist to the SiO2 layer without damaging the InP surface beneath the SiO2 layer. A typical SAG structure consists of a pair of mask stripes, as illustratively demonstrated in Fig. 3. In this work, the width (w) of the characterized SAG masks varies from 1 μm to 30 μm, with step-size of 1 μm, and the mask thickness is 210 (±10) nm. The gap (g) between the mask stripes is fixed as 20 μm. The SAG masks are aligned to be in parallel to the wafer major flat. Two neighboring mask pairs are placed far away from each other. After MOVPE SAG, the sample is characterized with a profilometer, scanning electron microscope (SEM) and micro-photoluminescence ($\mu$PL) spectroscopy.

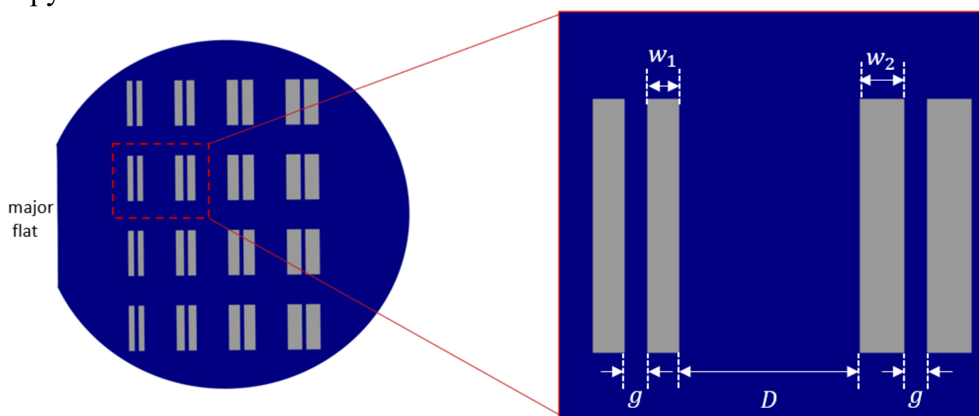


Fig. 3: An illustrative demonstration of the layout of the SAG masks(grey) on the InP substrate(blue). The demonstration is not in scale.

The SEM image in Fig. 4a shows the cleaved cross-section of the SAG mesa between two SiO2 masks. The grown semiconductor layer near the SAG mask is slightly thicker than that far away

from the mask, forming a tiny bump at the edge of the mesa. The bumps (i.e., overgrowth) near the mask are caused by the surface diffusion (on mask) of III group precursors. The plateau of the grown InP/InGaAsP mesa is 17 µm wide, providing enough tolerance for later fabrication. Fig. 4b zooms in to the left boundary of the SAG mesa. A slope with about 50° and overgrowth of 125 nm is observed at the immediate vicinity of the mask.

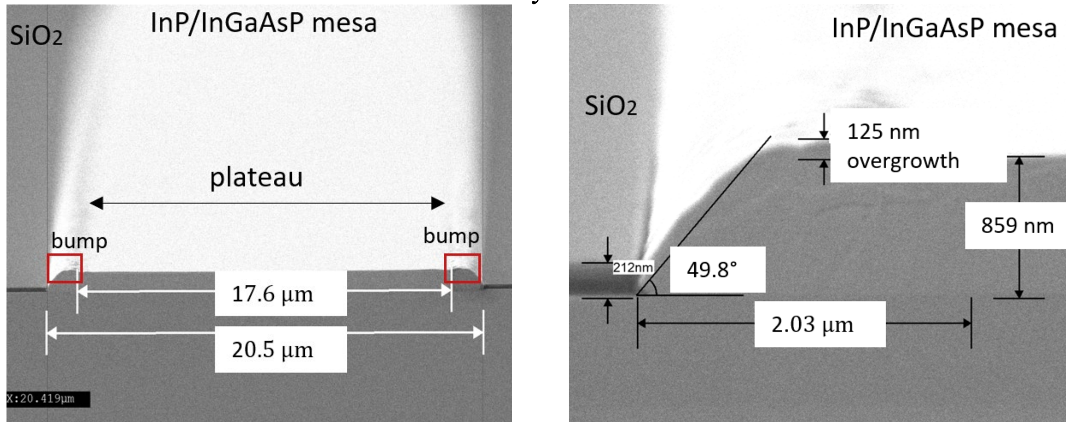


Fig. 4: a.(left) SAG mesa with a wide plateau; b.(right) zoom-in on the SAG mask/mesa boundary

GRE is determined by calculating the ratio of the thicknesses in the grown layer between the SAG mask stripes and far away from them. According to the topographical characterization using a surface profiler, GRE increases linearly with respect to the mask width, behaving similarly to the simulations, as shown in Fig. 5a. Besides, the actual effective diffusion length of the grown semiconductor material can be concluded as around 25 µm from Fig. 5a. The characterization results of samples from 4 independent fabrication runs demonstrate the repeatability of this work.

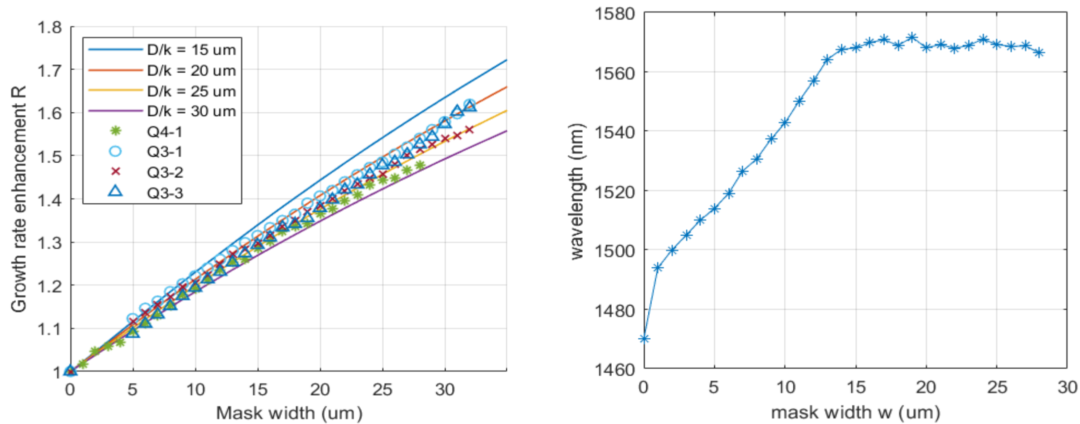


Fig. 5: a.(left) data from 4 independent growths (dots) proves a repeatable and controllable GRE control and good consistency with simulations (lines); b.(right) bandgap wavelength of SAG mesa depends linearly on mask width smaller than 15 µm

## Conclusion and Future Developments

In this work, we realized a controllable bandgap engineering approach based on SAG, resulting in a beyond 100 nm PL wavelength tuning with the standard core layer of InP Membrane on Silicon (IMOS) platform for the first time. In the next step, device fabrication using SAG technique can proceed further.

## Acknowledgement

This work was supported by the H2020 ICT TWILIGHT Project (contract No. 781471) under the Photonics PPP [8].

## Reference:

[1] F. Lemaitre, et al., “Multi-Band Gap Electro-Absorption Modulator Array in a Generic Integration Platform using Selective Area Growth,” in 21st European Conference on Integrated Optics (ECIO), 2019

[2] T. Fujii et al., "8-ch, 160-nm-Wavelength-Range Membrane Laser Array Using Selective Epitaxy on InP-on-Insulator Substrate," 2021 Optical Fiber Communications Conference and Exhibition (OFC), 2021, pp. 1-3.

[3] J. Decobert, et al., "AlGaInAs selective area growth for high-speed EAM-based PIC sources," 2013 International Conference on Indium Phosphide and Related Materials (IPRM), 2013, pp. 1-2,

[4] T.F.Kuech, “Metal-organic vapor phase epitaxy of compound semiconductors,” Material Science Reports, vol.2, Issue 1, 1-49, 1987

[5] L.A. Coldren, et al., Diode lasers and photonic integrated circuits, Wiley, App. A1.2,p511-p515, 2012

[6] Y. Jiao et al., “Indium phosphide membrane nanophotonic integrated circuits on silicon,” physica status solidi (a) 217.3 (2020): 1900606.

[7] D.G. Coronell et al., “Analysis of MOCVD of GaAs on patterned substrates,” Journal of Crystal Growth, vol.14, Issue 4, 581-592, 1991

[8] Spyropoulou, Maria, et al. "Towards 1.6 T datacentre interconnect technologies: the TWILIGHT perspective." Journal of Physics: Photonics 2.4 (2020): 041002.